

Carbon-in-silica composite selective solar absorbers: a determination of composition and dielectric properties

G Katumba^{*a} and A Forbes^{a,b,c}

^a CSIR-National Laser Centre, P O Box 395 Pretoria 0001, South Africa

^b School of Physics, University of Kwa Zulu-Natal, Private Bag X54001, Durban 4000, South Africa

^c Department of Physics, Stellenbosch University, Private Bag X1, Matieland 7602, South Africa

ABSTRACT

The Bruggeman and Maxwell-Garnett effective medium approximations have been used widely to investigate optical properties of many different composite materials. In most cases, the effective medium approximation assumptions are based on random unit cell models in which some metal particles are embedded in a dielectric medium. The shapes of the embedded particles can be varied between spherical, ellipsoidal and cylindrical shapes. A new and interesting structure of connected short chains of completely amorphous carbon intermixed with short chains of silica at nanoscale level has been observed recently. A generalised Bergman representation based on an arbitrary spectral density function is currently applied on these carbon-in-silica samples with a reasonable success of fitting between experiment and theory. The curve-fitting procedure adopted here has resulted in information such as volume fraction of carbon relative to silica, percolation threshold, the thickness and effective dielectric function of the composite layer.

Keywords: Bruggeman, Maxwell-Garnett, Bergman, effective medium approximations, nanoscale

1. INTRODUCTION

The Bruggeman and Maxwell-Garnett effective medium approximations have been used widely to investigate optical properties of many different composite materials. In most cases, the effective medium approximation assumptions are based on random unit cell models in which some metal particles are embedded in a dielectric medium. The shapes of the embedded particles can be varied between spherical, ellipsoidal and cylindrical shapes. A new and interesting structure of connected short chains of completely amorphous carbon intermixed with short chains of silica at nanoscale level has been observed recently. Attempts to apply the Bruggeman, Maxwell-Garnett and Bergman bounds effective medium formulations have proved to be unsatisfactory for the determination of the dielectric properties of the carbon-in-silica short-chain composites deposited on aluminium substrates. A generalised Bergman representation based on an arbitrary spectral density function is currently applied on these carbon-in-silica samples with a reasonable success of fitting between experiment and theory. The curve-fitting procedure adopted here has resulted in information such as volume fraction of carbon relative to silica, percolation threshold, the thickness and effective dielectric function of the composite layer.

2. THEORY

The optical constants of inhomogeneous composite media consisting of small particles hosted in a dielectric matrix can be derived from the optical constants of the homogeneous constituents. If the size of the homogeneities is much less than the wavelength of the incident light, then the electric and magnetic fields are almost constant over this characteristic length. With this quasi-static approximation, it is possible to describe the response of a composite material to an electromagnetic field by the dielectric function and magnetic permeability. In the solar and infrared wavelength regions,

* gkatumba@csir.co.za; phone +27 12 841 2660; fax +27 12 841 3152; www.csir.co.za

the magnetic permeability approaches unity and the optical properties can be treated with an effective dielectric function of the medium on the basis of effective medium approximations (EMAs).

The relationship between electric displacement, D , and electric field, E , for electrostatic fields and heterogeneous material is expressed as [1]:

$$D(x, y, z) = \varepsilon(x, y, z)E(x, y, z), \quad (1)$$

where $\varepsilon(x,y,z)$ is the dielectric function at the position (x,y,z) within the material. The effective dielectric function ε_{eff} for an inhomogeneous medium is defined by [1]:

$$\int_V D(x, y, z)dV = \int_V \varepsilon(x, y, z)E(x, y, z)dV = \varepsilon_{eff} \int E(x, y, z)dV, \quad (2)$$

where $D(x,y,z)$, $\varepsilon(x,y,z)$, $E(x,y,z)$ and dV are the local displacement, local dielectric function, local electric field and volume element, respectively. In the derivation of an effective dielectric function, each particle in the composite is considered to be embedded in an effective medium with the composite consisting of two or higher components.³¹ The usual procedure is then to make reasonable assumptions concerning the shape, size and distribution of the particles in the medium to obtain an analytical expression of the effective dielectric function in terms of volume fractions f_i ($i = 1, 2, 3, etc.$) and dielectric functions ε_i ($i = 1, 2, 3, etc.$) of the individual components, where i is the number of components in the composite medium. The most commonly used EMAs are the Maxwell-Garnett and Bruggeman models.^{26, 28} Discussion of the Maxwell-Garnett and Bruggeman EMA is presented here. Further, Bergman-Milton and the generalized Bergman representations of an EMA are also used in the discussion of results.

The Maxwell-Garnett EMA, in its simplest form, assumes that the medium has a separated-grain structure shown in Fig. 1(a). The Bruggeman model applies to a two-component medium having aggregate microstructure as shown in Fig. 1(b). The difference in microstructures between these models results in different modelled optical properties of the composite. The explicit microstructures help in the calculation of the effective dielectric function of the composite. The effective dielectric functions so obtained are often good approximations for many practical materials.

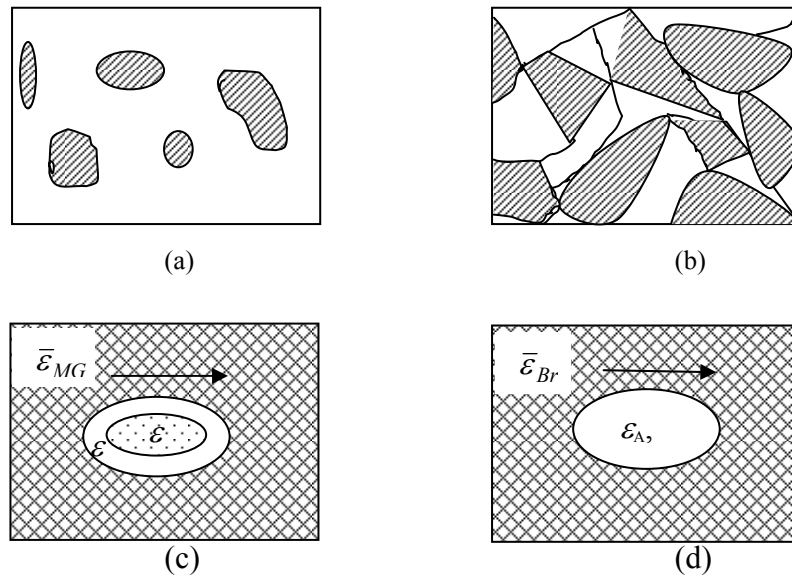


Fig. 1. Microstructures of (a) Separated-grain microstructure, (b) aggregate microstructure for a two-component medium, (c) Random Unit Cell corresponding to separated-grain structure used in Maxwell-Garnett model, (d) Random Unit Cell corresponding to aggregate structure used in the Bruggeman model.

The calculation of the effective dielectric function can be simplified by using Random Unit Cell (RUC) models that properly account for the essential features of the separate and aggregate microstructures as shown in Figs. 1(c) and 1(d), respectively. In the separated-grain microstructure of Fig. 1(c), the particles of material “A” are embedded in a continuous host material “B”. In the aggregate microstructure of Fig. 1(d), materials “A” and “B” enter on an equal footing to form a space-filling random mixture. The RUC can be spherical or non-spherical depending on the shape of the typical particle. The use of RUC models gives rise to a basic definition of an effective medium. It is a medium in which an embedded RUC should not be detectable in an experiment using electromagnetic radiation of a specific wavelength range [2]. This is an essential condition that allows the use of an optical theorem for absorbing medium. This theorem relates the extinction, C_{ext} , of the RUC compared to that of the surrounding medium to the scattering amplitude in the direction of the incident beam, $S(0)$, by [2]:

$$C_{ext} = 4\pi Re \left[\frac{S(0)}{k_\epsilon^2} \right], \quad (3)$$

with $k_\epsilon = 2\pi\bar{\epsilon}^{1/2} / \lambda$. Here k_ϵ denotes the wave vector amplitude in the effective medium of dielectric function, $\bar{\epsilon}$. From the basic definition of an effective medium it follows that $C_{ext} = 0$, and hence:

$$S(0) = 0, \quad (4)$$

which is the fundamental property of an effective medium.

The Bruggeman EMA, which considers the aggregate structure, may be introduced by expanding equation (4) in terms of the size parameter ka . By considering only the first order expansion, the forward scattering amplitude for an ellipsoid of semi-axes a_j ($j = 1, 2, 3$) is examined. The RUC of Fig. 1(d) for an ellipsoid aligned with the applied electric field polarised along one of the principal axes is used. The first order expansion of equation (4) yields:

$$S_j(0) = ik^3 \frac{a_1 a_2 a_3}{3} \left[\frac{\epsilon - \bar{\epsilon}}{\bar{\epsilon} + L_j(\epsilon - \bar{\epsilon})} \right] = 0 \quad (5)$$

where ϵ is the dielectric function of either of the constituents A or B, $\bar{\epsilon}$ is the average dielectric function of the effective medium and L_j is the depolarisation factor along the field. L_j should satisfy the conditions:

$$0 \leq L \leq 1 \text{ and } L_1 + L_2 + L_3 = 1. \quad (6)$$

Constituent materials “A” and “B” are treated symmetrically and each ellipsoid is taken to be embedded in the effective medium as shown in Fig. 1(d). An implicit equation for the Bruggeman effective dielectric function, $\bar{\epsilon}_{Br}$, can be obtained from equations (5) and (6), as [2]:

$$f_A \frac{\epsilon_A - \bar{\epsilon}_{Br}}{\bar{\epsilon}_{Br} + L_j(\epsilon_A - \bar{\epsilon}_{Br})} + (1 - f_A) \frac{\epsilon_B - \bar{\epsilon}_{Br}}{\bar{\epsilon}_{Br} + L_j(\epsilon_B - \bar{\epsilon}_{Br})} = 0 \quad (7)$$

where f_A and $(1 - f_A)$ are the filling factors of components “A” and “B”, respectively. In an aggregate of particles randomly oriented it is plausible to assume an average value. The effective dielectric function for the three principal axes stated above becomes [2]:

$$\frac{1}{3} \sum_{j=1}^3 f_A \frac{\varepsilon_A - \bar{\varepsilon}_{Br}}{\bar{\varepsilon}_{Br} + L_j(\varepsilon_A - \bar{\varepsilon}_{Br})} + (1 - f_A) \frac{\varepsilon_B - \bar{\varepsilon}_{Br}}{\bar{\varepsilon}_{Br} + L_j(\varepsilon_B - \bar{\varepsilon}_{Br})} = 0 \quad (8)$$

Equation (8) is symmetric with respect to interchanged roles of material components. It therefore follows that the Bruggeman model does not strictly apply to a particulate medium since it is not possible to distinguish between the particles and the surrounding medium. Since the derivation is based on an aggregate microstructure it allows a high practical value for the filling factor f_A , which is usually needed for solar energy applications. It is quite easy to adapt the latter equation for the case of spherical particles by taking $L_j = 1/3$. This yields the Bruggeman EMA as [3]:

$$f_A \frac{\varepsilon_A - \bar{\varepsilon}_{Br}}{\varepsilon_A + 2\bar{\varepsilon}_{Br}} + (1 - f_A) \frac{\varepsilon_B - \bar{\varepsilon}_{Br}}{\varepsilon_B + 2\bar{\varepsilon}_{Br}} = 0. \quad (9)$$

The generalised Maxwell-Garnett [4] model can be obtained by a similar expansion of equation (4). A separated-grain structure with a coated ellipsoid is shown in the RUC of Fig. 1(c). The Maxwell-Garnett effective dielectric function, $\bar{\varepsilon}_{MG}$, for this ellipsoidal RUC takes the form [5]:

$$\bar{\varepsilon}_{MG} = \varepsilon_B \frac{\varepsilon_B + L_j^A(\varepsilon_A - \varepsilon_B) + f_A(1 - L_j^B)(\varepsilon_A - \varepsilon_B)}{\varepsilon_B + L_j^A(\varepsilon_A - \varepsilon_B) - f_A L_j^B(\varepsilon_A - \varepsilon_B)} \quad (10)$$

where L_j^A and L_j^B are the depolarisation factors along the applied field for the inner and outer ellipsoid, respectively.

The latter equation is valid for low filling factor of particles, typically $f_A \leq 0.4$ because particle interactions are not taken into account in an explicit manner [2]. If particles are spherical, the Maxwell-Garnett EMA becomes:

$$\bar{\varepsilon}_{MG} = \varepsilon_B \frac{\varepsilon_A + 2\varepsilon_B + 2f_A(\varepsilon_A - \varepsilon_B)}{\varepsilon_A + 2\varepsilon_B - f_A(\varepsilon_A - \varepsilon_B)}. \quad (11)$$

A further attempt has been made to compare the experimental to the Bergman-Milton bounds formulated by Aspnes [6] and discussed by Niklasson [7]. The effective dielectric permeability for a two-phase composite of separate dielectric functions ε_A and ε_B and fill factors f_A and f_B , respectively, is given by:

$$\varepsilon_{BM} = \frac{\varepsilon_A \varepsilon_B + 2\varepsilon_h(f_A \varepsilon_A + f_B \varepsilon_B)}{2\varepsilon_h + f_A \varepsilon_B + f_B \varepsilon_A} \quad (12)$$

with the bounds,

$$\varepsilon_{host} = x\varepsilon_A + (1 - x)\varepsilon_B \quad (13)$$

The quantity ε_{host} is the dielectric function of the host material in which phases A and B are embedded.

The Bergman representation [8 - 10] of effective dielectric functions is the most general form of effective medium theories. The effective dielectric function, ε_{eff} , is expressed in the form of equation (14):

$$\varepsilon_{eff} = \varepsilon_M \left(1 - f \int_0^1 \frac{g(n, f)}{t - n} dn \right) \quad (14)$$

where the function $g(n,f)$ is called the spectral density which contains all topological details of the micro-geometry of the composite layer and f is the volume fraction of the embedded material. The spectral density is a real and non-negative function that is normalised for n in the interval $[0, 1]$. In equation (14) t is given by the expression:

$$t = \frac{\varepsilon_M}{\varepsilon_M - \varepsilon}. \quad (15)$$

In the case of an isotropic medium there is a condition for the first moment of the spectral density given by:

$$\int_0^1 g(n, f) dn = 1, \text{ and } \int_0^1 n g(n, f) dn = \frac{1-f}{3}. \quad (16)$$

This generalised Bergman formalism has proved useful in the investigations of two-phase composite materials. Here the goal has been to fit theoretical optical spectra of systems with known optical constants of the particle and matrix materials to experiment by the adjustment of $g(n,f)$. In many cases, an important property of the micro-geometry is the degree of connectivity of the embedded particles which enters in other formalisms as the percolation strength. It is well known that metal-insulator composites can switch between metallic and dielectric behaviour depending on the percolation strength. It can be shown that this feature shows up in the spectral density function $g(n,f)$ as a δ -function at $n=0$. This makes it possible to separate the spectral density into a diverging and a continuous part as follows:

$$g(n, f) = g_0(f)\delta(n) + g_{cont}(n, f), \quad (17)$$

where $g_0(f)$ is called the percolation strength. Therefore the fitting procedure involves three parameters, namely, volume fraction f , percolation strength $g_0(n,f)$ and n being an arbitrary number of points that are used to define the shape of $g(n)$ by a cubic spline interpolation.

3. EXPERIMENT

The preparation of samples is reported elsewhere [11 - 14]. Four types of nanosize carbon-containing coatings on aluminium substrates were investigated; *viz*, TEOS, TEOS+MTES, TEOS+AC₂O and TEOS+SOOT, where TEOS is a silica precursor. Total hemispherical reflectance measurements in the 400 to 2400 nm wavelength range were performed on the samples using a Varian Cary 500 spectrophotometer. The instrument is equipped with a 110 mm integrating sphere coated with polytetrafluoroethylene (ptfe) material. A spectralon reference was used at 4 nm resolution. These reflectance measurements were corroborated by measurements from a Perkin Elmer Lambda 900 spectrophotometer.

High resolution cross-sectional transmission electron microscopy (HR-XTEM) was used to determine the microstructure of the samples. Electron energy loss spectroscopy (EELS) was used to observe the qualitative distribution of the carbon particles in the silica matrix.

The various EMAs discussed above were then used for fitting to the experimental reflectance measurements. The fitting procedure output the carbon particle volume fraction, the dielectric function, the thickness and the simulated reflectance spectrum of the composite layer on a 2 mm aluminium substrate.

4. RESULTS AND DISCUSSION

The microstructure of the samples was studied by cross-sectional high resolution transmission electron microscopy (X-HRTEM). A representative X-HRTEM image is shown in Fig. 2.

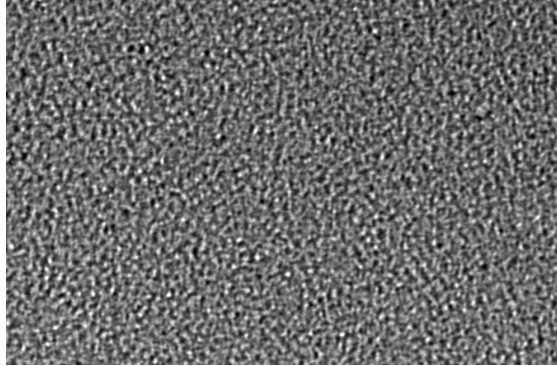


Fig. 2. A typical X-HRTEM image of C-SiO₂ composite showing the chain-like fine structure.

Some typical theoretical reflectance calculations for various film thicknesses in the Bruggeman, Maxwell-Garnett and the Bergman-Milton EMA formalisms are compared with experiment in Figs. 3 to 5, respectively. There is evident disparity in all the three comparison fit attempts.

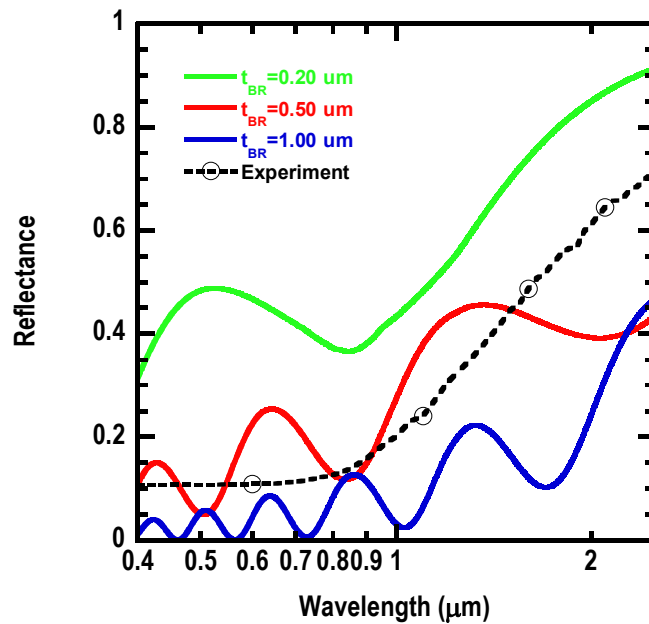


Fig. 3. Comparison of Bruggeman EMA with fill factor 0.33 to experiment. There is great disparity between theory and experiment for many other fill factors and coating thicknesses.

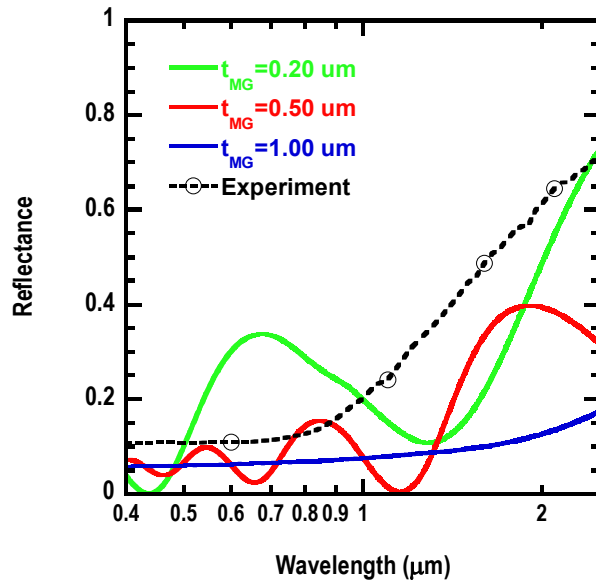


Fig. 4. Comparison of the Maxwell-Garnett EMA with fill factor 0.33 to experiment. There is great disparity between theory and experiment for many other fill factors and coating thicknesses.

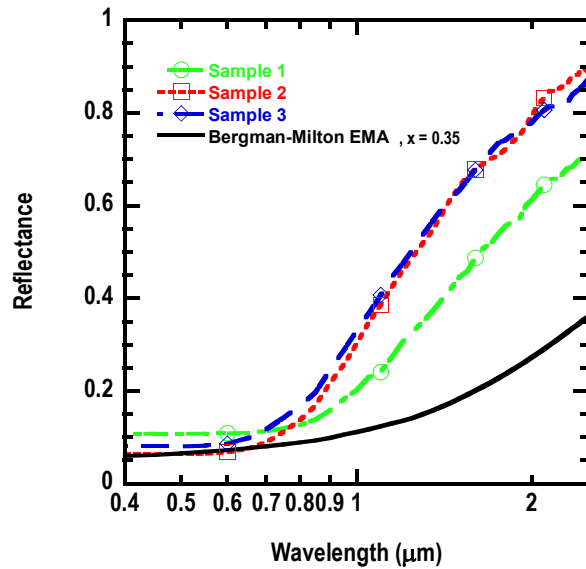


Fig. 5. The Bergman-Milton bounds EMA compared with experiment for $x=0.35$. There is great disparity between theory and experiment for many other fill factors and x parameter values.

The Bergman representation fits to reflectance measurements of three samples are shown in Fig. 6. There is evidence of successful matching of experiment and theory in this approach. The parameters extracted from the curve-fitting are presented in Table 1. Independent measurements of some of the parameters, where possible, have been made for comparison; these are also presented in Table 1.

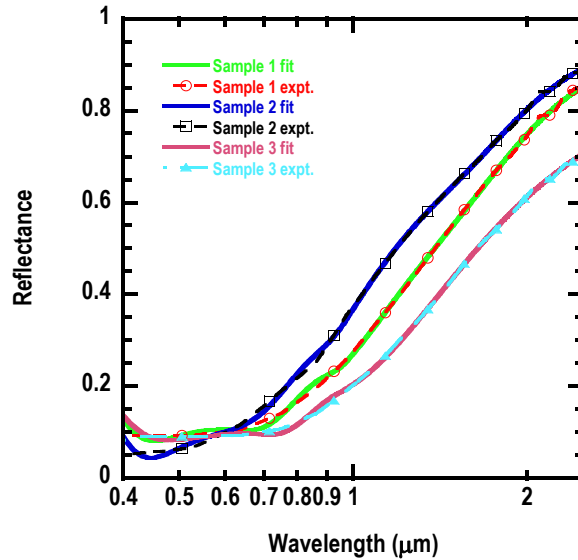


Fig. 6. The Bergman representation fitted to experimental data. There is agreement between theory and experiment.

It is clear from Table 1 that the fit parameters are agreeing with the independent measurements within the experimental error range.

Table 1. Data extracted from the Bergman fit. There is agreement within experimental limits between the fit values and the independent measurements.

Sample	Fit thickness (μm)	TEM thickness (μm)	Fit carbon vol. fraction	Carbon vol. fraction (LIBS)	Percolation threshold
1	1.02	1.14	0.33	0.32	0.51
2	1.12	1.00	0.28	0.29	0.54
3	0.87	0.92	0.35	0.37	0.55

5. CONCLUSIONS

The Bergman EMA representation has been fitted successfully to composite coatings of carbon nano-chains embedded in silica. Film thickness, carbon volume fraction and percolation threshold were extracted.

ACKNOWLEDGEMENTS

Swedish International Development Agency (SIDA) and the Swedish Agency for Research Cooperation (SAREC) funded the research work. University of Zimbabwe (UZ) and the African Laser Centre (ALC) provided subsistence and travel funds.

REFERENCES

- [1] Wäckelgård, E., Niklasson, G.A. and Granqvist, C.G., *Selectively solar-absorbing coatings (Chapter 3), in Energy-The State of the Art*. London: James & James (Science Publishers) Ltd. (2001).
- [2] Niklasson, G.A., *Optical Properties of Inhomogeneous Two-component Materials, in Materials for Solar Energy Conversion System* (edited by Granqvist, C.-G.). Oxford: Pergamon Press (1991).
- [3] Bruggeman, D.A.G., Berechnung verschiedener physikalischer konstanten von heterogenen substanzen. *Ann. Phys.*, **24**, 636 – 679 (1935).
- [4] Garnett, J.C.M., Colours in metal glasses and in metallic films. *Phil. Trans. R. Soc. Lond.*, **203**, 385 – 420 (1904).
- [5] Niklasson, G.A. and Granqvist, C.-G., Optical Properties and Solar Selectivity of Coevaporated Co-Al₂O₃ Composite Films. *J. Appl. Phys.*, **55**, 3382 – 3410 (1984).
- [6] Aspnes, D.E., Optical Properties of thin Films. *Thin Solid Films*, **89**, 249 – 262 (1982).
- [7] Niklasson, G.A., Co-Al₂O₃ Selective Solar Absorbing Films: Structure and Effective Medium Theory for the Optical Properties. *Solar Energy Materials*, **17**, 217 – 226 (1998).
- [8] Weissker, H.-Ch., Furthmüller, J., & Bechstedt, F., Validity of effective-medium theory for optical properties of embedded nanocrystallites from *ab initio* supercell calculations. *Phys. Rev. B* **67**, 165322-1/5 (2003).
- [9] Bergman, D., The dielectric constant of a composite material – a problem of classical physics. *Phys. Reports*, **43**, 377 – 407 (1978).
- [10] Theiss, W., SCOUT optical spectrum simulation, M. Theiss Hard- and Software, Aachen (2002).
- [11] Katumba, G., Lu, J., Olumekor, L., Westin, G. and Wäckelgård, E., Low cost selective solar absorber coatings: Characteristics of carbon-in-silica synthesized with sol-gel technique. *Journal of Sol-Gel Science and Technology*, **36**, 33 – 43 (2005).
- [12] G Katumba, L Olumekor, A Forbes, G Makiwa, B Mwakikunga, J Lu and E Wackelgard, *Optical, thermal and structural characteristics of carbon nanoparticles embedded in ZnO and NiO as selective solar absorbers*, *Solar Energy Materials & Solar Cells*, **92**, 1285-1292 (2008).
- [13] G. Katumba, B. W. Mwakikunga and T. R. Mothibinyane, *FTIR and Raman spectroscopy of carbon nanoparticles in SiO₂, ZnO and NiO matrices*, *Nanoscale Research Letters*, **3**, 421-426 (2008).
- [14] G Katumba, G Makiwa, T R Baisitse, L Olumekor, A Forbes and E Wackelgard, *Solar selective absorber functionality of carbon nanoparticles in SiO₂, ZnO and NiO matrices*, *Phys. Stat. sol. (c)* **5**, 549-551 (2008).